

Adversarial Open Set Domain Adaptation Based on Mutual Information

Tasnia Shermin, Guojun Lu, *Senior Member, IEEE*, Ferdous Sohel, *Senior Member, IEEE*, Shyh Wei Teng, and Manzur Murshed, *Senior Member, IEEE*

Abstract—Domain adaptation focuses on utilizing a labeled source domain to classify an unlabeled target domain. Until recently domain adaptation setting was attributed to have only shared label space across both domains. However, this setting/assumption does not fit the real-world scenarios where the target domain may contain label sets that are absent in the source domain. This circumstance paved the way for the *Open Set Domain Adaptation* (OSDA) setting that supports the availability of unknown classes in the domain adaptation setting and demands the domain adaptation model to classify the unknown classes as an unknown class besides the shared/known classes. Negative transfer is a critical issue in *open set domain adaptation*, which stems from a misalignment of known/unknown classes before/during adaptation. Current open set domain adaptation methods lack at handling negative transfers due to faulty known-unknown class separation modules. To this end, we propose a novel approach to OSDA, *Domain Adaptation based on Mutual Information* (DAMI). DAMI leverages the optimization of *Mutual Information* to increase shared information between known-known samples and decrease shared information between known-unknown samples. A weighting module utilizes the shared information optimization to execute *coarse-to-fine* separation of known and unknown samples and simultaneously assists the adaptation of known samples. The weighting module limits negative transfer by step-wise evaluation and verification. DAMI is extensively evaluated on several benchmark domain adaptation datasets. DAMI is robust to various openness levels, performs well across significant domain gaps, and remarkably outperforms contemporary domain adaptation methods.

Index Terms—Open set domain adaptation, adversarial domain adaptation networks, mutual information.

I. INTRODUCTION

Deep neural networks exhibit remarkable performance in computer vision tasks. However, they require a bulk of annotated training data and the same underlying distribution for training and testing data to perform optimally [1], [2]. The scarcity of labeled data and the lack of ability to overcome domain discrepancy [3], [4], [5] through generalization have motivated Domain Adaptation (DA) works. Domain adaptation works concentrates in adapting a model to an unlabeled target domain which has access to a labeled source domain [6], [7], [8], [9], [10], [11], [12], [13], [14], [15]. Early domain adaptation works followed the *closed set* assumption that there exist only common label sets across the source and

Tasnia Shermin, Guojun Lu, Shyh Wei Teng, and Manzur Murshed are with the School of Science, Engineering and Information Technology, Federation University, Churchill-3842, Australia (email: {t.shermin, guojun.lu, shyh.wei.teng, manzur.murshed}@federation.edu.au)

Ferdous Sohel is with Murdoch University, WA-6150, Australia (email: f.sohel@murdoch.edu.au)

target domains [9], [16], [17]. For modifying this unrealistic assumption, *open set* domain adaptation is recently studied. Open Set domain adaptation by Back-Propagation (OSBP) [18] focuses on having unknown classes in the target domain only while [19] proposes to consider unknown samples in both the domains. In this work, we focus on the setting proposed by Saito et al. [18], as shown in Figure 1.

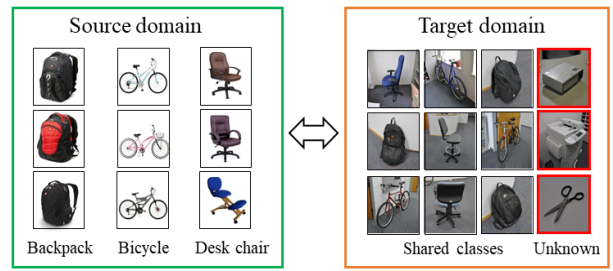


Figure 1: Open set domain adaptation setting introduced by Saito et al. [18].

The task in open set domain adaptation is to draw a boundary between known and unknown classes as correctly as possible without any prior information about the unknown classes. Then adapt the known classes in the target domain to the source domain. The main challenge of open set domain adaptation is the negative transfer. Due to the misalignment of known or unknown target samples during domain adaptation, for some tasks Open set domain adaptation models perform worse than non-domain adaptation classifier trained only on the source domain [19], [13], [20]. This notion of performance loss by a domain adaptation model is termed as negative transfer [21].

It is required to separate the unknown target samples and align only the known target samples to the source domain to mitigate negative transfer. Many authors have sought to depend only on source-trained multi-binary classifiers for separating known-unknown target samples [20], [22]. However, such classifiers may suffer from the overconfidence issue [23] and yield high confidence for unknown target samples. This way unknown samples will be treated as known samples at the time of separation and motivate negative transfer. On the other hand, Towards Inheritable Models (TIM) [24] trains a model on the source domain and self-generated out-of-source-distribution samples to ease the overconfidence issue. Later uses this trained source model for adapting known classes and rejects unknown classes by aligning the unknown classes to the generated out-of-source-distribution samples. However,

this approach may initiate negative transfers by confining the unknown domain similar to [19]. Clearly, an open set domain adaptation model with a faulty known-unknown samples identification module is vulnerable to negative transfer.

However, in this work, instead of relying only on a source trained network for separating known-unknown samples, we concentrate in training a separating module to learn to group known classes across domains together and simultaneously separate unknown classes. We fulfill this objective by increasing shared information between source-known and target-known samples, and decreasing shared information between source-known and target-unknown samples. For exploring shared information, we leverage *Mutual Information* (I), which is capable of quantifying the amount of information obtained about one random variable by observing the other random variable.

We refer to our proposed open set domain adaptation model as Domain Adaptation based on Mutual Information (DAMI). DAMI employs a three-step known-unknown separation weighting module before adversarial domain adaptation: (1) Coarse Separation Network (CSN), (2) Mutual Information Optimization Network (MION), and (3) Fine Separation Network (FSN). First, CSN draws a coarse boundary between tentative known and unknown target samples. Then, based on the decision of CSN, MION learns richer domain discriminative features through optimizing *Mutual Information* between known-unknown target samples and source samples. This optimization relaxes the overconfidence constraint of the MION by enforcing the unknown target samples to move away from known samples and encourages positive transfer in the latter step.

Finally, for finely separating unknown target samples from known samples, FSN utilizes the features of MION and assess the *Point-wise Mutual Information* (pmi) between each target samples and the source domain, which is a measure of co-occurrence. Upon finishing its iteration, FSN assigns identifiable weights to known and unknown target samples. The assigned weights are further used for finally rejecting unknown samples and adapting the known samples adversarially. The three-step assessment ensures that our model encourages well separation of known samples from unknown samples. As a result, DAMI assists in a better adaptation of known target samples to the source domain. DAMI outperforms the contemporary methods and non-DA classifiers, which indicates the mitigation of negative transfer. A pictorial outline of DAMI is shown in Figure 2.

The key contributions of this work can be summarized as:

- We propose a novel open set domain adaptation model that limits negative transfer by easing the overconfidence issue of deep networks through manipulating shared information between known-unknown target samples and the source domain.
- We discuss in detail the theoretical insights behind designing DAMI.
- We present extensive empirical evaluation on several datasets to demonstrate superior state-of-the-art performance of DAMI compared to contemporary domain adaptation models.

II. RELATED WORK

A. Closed Set Domain Adaptation

In Closed set domain adaptation methods, the focus is to reduce the divergence between the source and the target domains. The build-out of recent closed set domain adaptation methods based on deep learning models [25], [13], [17], [26], [10], [27], [28], [15], [29] originate from the prevalent shallow domain adaptation methods [30], [31], [32], [33], [34], [35]. Domain adaptation methods based on closed set domain adaptation setting can be grouped into three different categories. The first one is based on static moment matching, such as Maximum Mean Discrepancy (MMD) [36], [26], [17], [27], Central Moment Discrepancy (CMD) [37], and second-order statistics matching [38]. The second category of methods utilizes the Generative Adversarial Networks (GAN) [39] for initiating the generation of images that are non-discriminative to the shared label space of both domains [29], [16], [10], [13]. Domain adversarial methods that align pixels and features from both domains and recreate labeled target images for data augmentation also fall into this category [40], [41], [42], [43], [44], [9]. Furthermore, Cycle-Consistent GAN [45] is used for developing CycleGAN-based [46], [47], [48] domain adaptation methods. The last category of methods exploits Batch Normalization statistics for adapting domains [49], [50].

B. Open Set Domain Adaptation

Assign-and-Transform-Iteratively (ATI) [19] follows the open set domain adaptation setting which has unknown classes in both the domains. ATI evaluates the distance of each target sample from the core of every source class, aligns target samples residing in near vicinity to known classes and rejects unknown target samples by aligning them towards the unknowns of the source domain. Open Set Back-Propagation (OSBP) [18], on the other hand, implements a generative adversarial domain adaptation model. Both ATI and OSBP approaches require some threshold hyper-parameters to distinguish between known and unknown classes. Since this threshold hyper-parameters are not learnable or adaptive, they encourage negative transfer by aligning known samples to the ‘unknown’ class.

However, Separate to adapt (STA) [20] utilizes underlying domain similarity of target samples for progressive separation of known-unknown target samples before domain adaptation. STA is still exposed to misalignment of unknown samples for relying only on the decision of a multi-binary classifier. Similar to STA, Mutual to Separate (MTS) [22] employs a multi-binary classifier with a domain adversarial network to separate unknown samples and simultaneously adapt shared classes across both domains. MTS proposed mutual learning between the separation network and the adaptation network based on the distance between the features of both networks. Unlike MTS, DAMI leverages *Mutual Information* for distinguishing known-unknown samples and provides the adversarial module only with instance-level weights for adaptation.

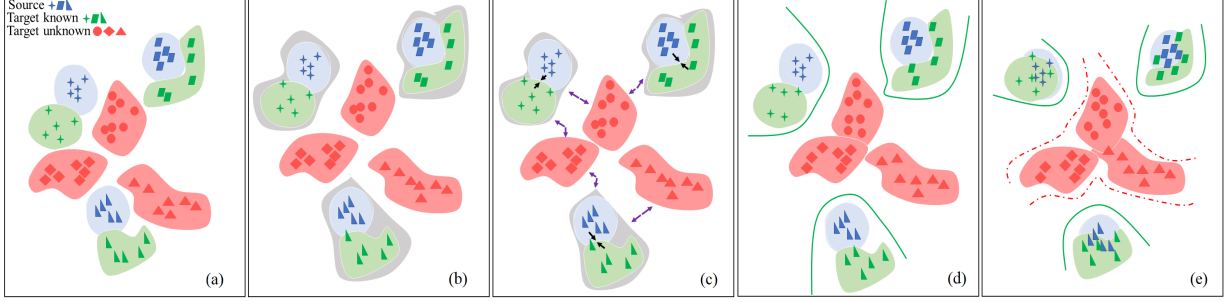


Figure 2: An overview of the proposed DAMI approach. (a) A view of an initial state of the open set domain adaptation setting. (b) The situation at the end of the first step of separating module, CSN roughly determines the similarity between target samples and source samples. (c) After the second step, due to optimizing shared information, the features of unknown classes are pushed away from known classes (purple arrows) and the shared information between known source and known target classes increases (black arrows) in the MION. (d) In the final step, after verifying the known and unknown samples based on their co-occurrence probability pmi to the source domain, the FSN utilizes the latent space created between the known and unknown domain in the MION to draw a fine boundary between known and unknown samples. (e) Based on the generated weights w from FSN, the main feature discriminator aligns known samples to source domain, and the main classifier constructs boundary between known classes and the ‘unknown’ class.

C. Mutual Information and Domain Adaptation

Leveraging information as a basis to learn representations using paired data has been explored in domain adaptation [51], co-clustering and others [52], [53]. These mentioned works are constructed by utilizing several information bottleneck principles [54], [55], [56]. For unsupervised *closed set* domain adaptation, DADA [57] minimizes I for disentangling features. For learning representations, DeepINFOMAX [58] maximizes I between compact and spatially-preserved features, IMSAT [59] maximizes I between samples and their representations for better learning. IIC [60] maximizes I between the sample and its distorted version for clustering. Unlike above-mentioned works, DAMI leverages optimization of information for better discriminating known and unknown classes. DeepINFOMAX and IMSAT requires a complex neural estimator for computing I over continuous random variables. In contrary, IIC computes I for discrete random variables. Similar to DADA, DAMI leverages MINE [61] for estimating *Mutual Information*.

III. PROPOSED METHODOLOGY

In this section, we formally describe the open set domain adaptation setting of our interest and present our proposed method.

A. Domain Adaptation Setting

The open set domain adaptation setting of our focus constitutes a source domain $D_s = (x_i^s, y_i^s)_{i=1}^{n_s}$ of n_s labeled instances associated with $|C_s|$ classes, which are drawn from distribution p_s and a target domain $D_t = (x_j^t)_{j=1}^{n_t}$ of n_t unlabeled instances drawn from distribution p_t . We denote the class labels of the target and source domains as C_t and C_s respectively. The shared label space is denoted as $C = C_s \cap C_t$. $\bar{C}_t = C_t \setminus C$ represents the label sets private to the target domain, which should be recognized as ‘unknown’. In this type of open set domain adaptation, it is difficult to identify

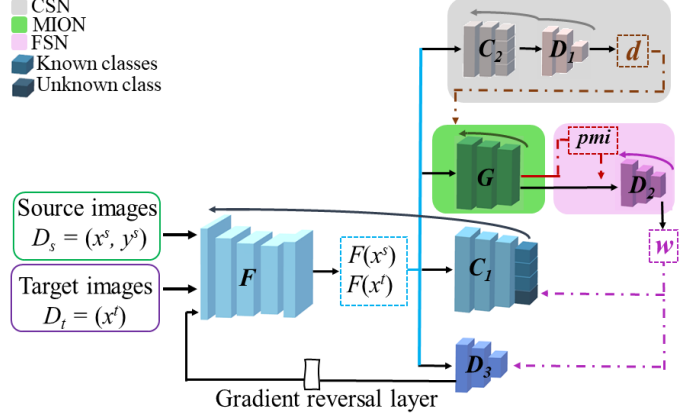


Figure 3: Block diagram of DAMI. The adversarial domain adaptation module comprises of the feature extractor F , main classifier C_1 , and adversarial domain discriminator D_3 . The weighting module is constructed with an auxiliary feature discriminator G , a multi-class one-vs-rest classifier C_2 , and two non-adversarial binary discriminators D_1 and D_2 . The final weights w for separating known and unknown target samples are generated after three-stage evaluation through (1) Tentative Separation Network (TSN), (2) Mutual Information Optimization Network (MION), and (3) Fine Separation Network (FSN). The adversarial domain adaptation module utilizes the weights w further to reject unknown target samples and align known target samples to the source domain. The right arrows denote forward passes, dotted arrows represent the evaluation of similarity measures, and left arrows to represent backward passes.

which part of the target label space C_t is shared with the source label space C_s because the target domain is fully unlabeled and C_t is unknown at the training time. It is challenging to differentiate between known and unknown target samples as we do not have any trace of the target sample labels.

B. Proposed Domain Adversarial Model

Our proposed method comprises of two modules: 1)Domain Adversarial Network (DAN) and 2) Weighting module for known-unknown separation.

1) *Domain Adversarial Network (DAN)*: The proposed method is illustrated in Fig. 3. We aim to construct a boundary between known and unknown target samples and reduce divergence between the source domain and the known samples of the target domain by learning transferable features in a two-player minimax game. In line with [28], [18], [20], we exploit generative adversarial domain adaptation. The first player of our model is a domain discriminator D_3 that is trained to distinguish the features of the source domain from the target domain. The second player is a feature generator F that is simultaneously trained to reduce feature distribution divergence in the opposite direction of the domain classifier. The ultimate objective is to train the source classifier C_1 to correctly classify known target samples to its corresponding class and target samples belonging to unknown classes as ‘unknown’.

The feature generator F takes inputs from both source domain D_s and target domain D_t . The classifier C_1 takes features from F and gives $|C| + 1$ dimensional output, i.e. the $|C|$ known classes in the source domain and an additional ‘unknown’ class for \overline{C}_t . During the forward pass, within C_1 , the features are transformed to a $|C| + 1$ -dimensional class probability through softmax function as, $\sigma(z) = \exp(z) / (\sum_{i=1}^{|C|+1} \exp(z_i))$, where z is the logit vector. We define the classification loss on the source domain as follows,

$$E_{C_1}^s = \frac{1}{n_s} \sum_{i=1}^{n_s} L_{C_1}(C_1(F(x_i^s)), y_i^s). \quad (1)$$

Here, L_{C_1} is the standard cross-entropy loss function for minimizing the error of the classifier C_1 .

For adversarially aligning the distributions of source and target data in the shared label space C , we utilize the adversarial domain discriminator D_3 . We propose to infuse the outputs of D_2 as instance-level weights (i.e. $w(x_j^t) = D_2(G(F'(x_j^t)))$), where a larger $w(x_j^t)$ implies a higher probability to be from the known classes (Section III-B2)) for target samples in the loss of the adversarial discriminator D_3 as,

$$E_{D_3} = -\frac{1}{n_s} \sum_{i=1}^{n_s} \log(D_3(F(x_i^s))) - \frac{1}{n_t} \sum_{j=1}^{n_t} w(x_j^t) \log(1 - D_3(F(x_j^t))). \quad (2)$$

The adversarial training between the feature extractor F and discriminator D_3 in this module is equivalent to aligning known target samples towards the source domain.

To preserve the characteristics of cluster assumption during adaptation, we further minimize the conditional entropy with respect to the known classes of the target domain as follows,

$$E_{ce}^t = \sum_{x_j^t \in D_t} w(x_j^t) L_{ce}^t. \quad (3)$$

Here, $L_{ce}^t = -\mathbb{E}_{x_j \sim D_t} [C_1(F(x_j))^\top \ln(C_1(F(x_j)))]$. Minimizing conditional entropy will enforce confidence on the classifier for unlabeled target data, and the decision boundaries will occur far away from the data-dense regions in the target domain. We incorporate our generated instance-level weights to the entropy minimization so that only the entropy of target samples estimated to be from the known classes are minimized. However, if the classifier has high capacity, only minimizing conditional entropy may result in over-fitting to the unlabeled samples. To prevent this, virtual adversarial training (VAT) [62] has been utilized in addition to conditional entropy minimization to smooth the classifier surface around the unlabeled points [62], [63]. In line with [63], we optimize the VAT loss with respect to both the source and target domain as follows,

$$E_v^t = \sum_{x_j^t \in D_t} w(x_j^t) L_{vat}^t. \quad (4)$$

$$E_v^s = L_{vat}^s.$$

Here, $L_{vat} = -\mathbb{E}_{x \sim D} [\max_{\|\gamma\| < \epsilon} \mathcal{D}_{KL}(C_1(F(x)) \| C_1(F(x + \gamma)))]$, \mathcal{D}_{KL} represents the Kullback–Leibler divergence and γ denotes perturbation. It is worth mentioning, we have used our generated weights in VAT losses for enforcing classifier to be consistent within the norm-ball neighborhood of each sample belonging to the shared label space C .

For training the classifier C_1 to recognize unknown target samples, we use the target samples which are assigned low weights by D_2 . Based on our weighting module, target samples with small weights ($w(x_j^t)$) have more probability of belonging to the unknown classes. We define the weighted loss for separating the ‘unknown’ class as,

$$E_{C_1}^t = \frac{1}{n_t} \sum_{j=1}^{n_t} w(x_j^t) L_{C_1}(C_1(F(x_j^t)), y_u^t). \quad (5)$$

where, y_u^t denote the label of the unknown class. Note that this loss is minimized with respect to only the ‘unknown’ index of the classifier C_1 .

2) *Weighting Module for Known-Unknown Separation*: In this section, we present the conceptual details of the weighting module of DAMI.

Overview: The main challenge in DAMI, as illustrated in Equations (1)–(5), is the way of measuring the similarity of target samples to the source domain on the basis of which the unknown target samples are to be rejected. We aim to develop a weight measure $w(x_j^t)$ for each target samples by employing a three-step evaluation procedure.

In the first step of the weighting module, CSN evaluates the underlying domain similarity of target samples to source domain with the help of a binary discriminator D_1 which depends on the decision of a source trained multi-class classifier C_2 and generates a similarity score d for each target sample. Afterwards, by using the similarity score d , the auxiliary feature discriminator G in MION manipulates the *Mutual Information* between tentative known-unknown target samples and the source domain. This facilitates G to drive tentative unknown samples away from the source domain by decreasing

shared information and draw tentative known samples closer to the source domain by increasing information in between them.

In the final step, FSN utilizes the output of the auxiliary feature discriminator G for selecting target samples with highest and lowest similarity to the source domain based on their average co-occurrence, i.e. *Point-wise Mutual Information (pmi)* to the source samples. The *pmi* verifies the similarity/dissimilarity of target samples to the source domain by providing a measure of the amount of shared information between them. Then, FSN uses the discriminative features of G to train another binary discriminator D_2 with the verified target samples to learn to finely separate known and unknown target samples and assign them high and low weights respectively. The final instance-level weights w are further used by DAN for adapting known samples and rejecting unknown samples.

Mechanism in Detail: For generating preliminary instance-level similarity score; first, we separate known and unknown target samples based on their underlying domain similarity to the source domain. To accomplish this, we place a multi-class one-vs-rest classifier C_2 (Fig. 3) which takes features from an auxiliary feature discriminator G and determines the similarity of target samples to individual known-source labels C_s . We utilize a leaky softmax [64] and binary cross-entropy loss to optimize C_2 as follows,

$$E_{C_2} = -\frac{1}{n_s} \sum_{i=1}^{n_s} \sum_{k=1}^{|C_s|} y_{i,k}^s \log(C_2^k(F(x_i^s))) + (1 - y_{i,k}^s) \log(1 - C_2^k(F(x_i^s))) \quad (6)$$

where, $C_2^k(F(x_i^s))$ is the probability of a sample belonging to the k^{th} known class. This classifier is trained only on the source domain which means the probability $C_2^k(F(x))$ can be seen as the similarity between the target sample and the known class k . The element-sum i.e. $E_{sum}(x) = \sum_{k=1}^{|C_s|} C_2^k(F(x))$ of the leaky-softmax outputs for samples resembling the source domain will be high or close to 1 whereas, samples dissimilar to source domain will yield low or close to 0 outputs. Thus, samples from known classes of the target domain are prone to producing a higher $E_{sum}(x)$. This indicates that known target samples tend to share underlying discriminative domain information with the source domain. On the other hand, unknown target samples produce low $E_{sum}(x)$, which represents more uncertainty in the class assignment. We further utilize the output of C_2 to train a binary discriminator D_1 for finely separating target samples similar to the source domain from samples dissimilar to the source domain. The binary discriminator assumes that known target samples belong to the shared label space. Therefore, D_1 trains itself to produce high output for samples which resemble source samples and low output for samples that have negligible or no similarity

with the source domain as follows,

$$E_{D_1} = -\frac{1}{n_s} \sum_{i=1}^{n_s} \log D_1(E_{sum}(x_i^s)) - \frac{1}{n_t} \sum_{j=1}^{n_t} \log(1 - D_1(E_{sum}(x_j^t))). \quad (7)$$

Now, the output $d(x_j^t) = D_1(E_{sum}(x_j^t))$ of D_1 can be used as an instance-level weight for target samples.

We introduce a feature discriminator G . The objective of placing the auxiliary feature discriminator G is to minimize the common information (*Mutual Information*) between unknown target samples and the source samples. And maximize the *Mutual Information* between known target samples and the source samples. Maximizing shared information between known target samples and source samples will increase the amount of uncertainty removed while assigning a class to target samples by knowing the source samples. On the other hand, minimizing shared information between unknown target samples and source samples will introduce more uncertainty in classifying the unknown target samples. In particular, knowing how to group similar classes together and simultaneously knowing how to separate different classes will limit the over-confidence of G for classifying unknown samples as known.

We rank the output of D_1 for target samples and identify m known and unknown target samples based on the highest and lowest similarity score ($d(x_j^t)$), where, $m = b/4$ and b = batch size. Note that the empirical value of m is found suitable for a wide range of tasks. In each batch, we utilize the selected m tentative known and m tentative unknown target samples for optimizing shared information. Since we obtain limited number of target samples after filtering the output of D_1 , we apply data augmentation which also imposes robustness in the optimization. We apply different transformations such as random crops, central crops and horizontal flips. The images within each batch are repeated to make sure that every source sample is paired with the original target sample and their transformations.

DAMI adopts the Mutual Information Neural Estimator (MINE) [61] to calculate the I . In DAMI, MINE exploits the bound $I(X^s; X^t) \geq I_\Theta(X^s; X^t)$, where X represents the features/output of G and $I_\Theta(X^s; X^t)$ denotes the *neural information measure*. The unbiased estimation of *Mutual Information* on l i.i.d samples is measured by using a neural network T_θ as,

$$\widehat{I(X^s; X^t)}_l = \sup_{\theta \in \Theta} \mathbb{E}_{P_{X^s X^t}^{(l)}} [T_\theta] - \log(\mathbb{E}_{P_{X^s}^{(l)} \otimes \widehat{P}_{X^t}^{(l)}} [\exp^{T_\theta}]) \quad (8)$$

here, $P_{X^s X^t}$ is the joint probability distribution of $(G(F(D_s)), G(F(D_t)))$, and $P_{X^s} = \int_{X^t} P_{X^s X^t}$ and $P_{X^t} = \int_{X^s} P_{X^s X^t}$ are the marginals. The objective of maximizing and minimizing I can be fulfilled by gradient ascent and descent respectively. The expectations are estimated by shuffling the samples from the joint distribution

within a batch, which also establishes dependency through marginalization. Therefore, G is trained to optimize I as,

$$\begin{aligned} E_{MI_k} &= \lambda_1 I(\widehat{X^s}; \widehat{X^t})_l \\ E_{MI_{uk}} &= \lambda_2 I(\widehat{X^s}; \widehat{X^t})_l \end{aligned} \quad (9)$$

Here, E_{MI_k} and $E_{MI_{uk}}$ represent the computed *Mutual Information* (Eqs. 8) of rough known and unknown target samples (evaluated by CSN) with the source domain respectively. The hyper-parameters (λ_1 and λ_2) are easy to choose empirically and work well across multiple tasks. Setting $\lambda_1 > \lambda_2$ ensures that I of known samples are given higher attention than unknowns.

After optimizing E_{MI_k} and $E_{MI_{uk}}$, G learns a function that partitions the data such that the features of source samples are closer to the known target samples than the unknown target samples. For the final fine separation of known and unknown target samples, we utilize the *Point-wise Mutual Information pmi* between target and source samples based on the output of G . To convert the output of G to probability distribution we use a softmax layer. The softmax outputs of G for the whole batch of a target (Z^t) and source data (Z^s) (without any transformed version) can be treated as a distribution of discrete random variables. *Point-wise Mutual Information* between two instances (Z_i^s and Z_j^t) of two random variables (Z^s and Z^t) represents the probability of their co-occurrence compared to their individual or independent occurrence. *Point-wise Mutual Information* can be formalized as,

$$pmi(Z_i^s; Z_j^t) = \log \frac{P(Z_i^s, Z_j^t)}{P(Z_i^s)P(Z_j^t)}. \quad (10)$$

The dependency between Z^s and Z^t is ensured by marginalization over a batch. The joint probability distribution is constructed as $M = Z^s \cdot Z^t^\top$ ($n_s \times n_t$ tensor M), where Z^s and Z^t matrices hold the dimension of $n \times C_s$. The marginals are computed from the summation of rows and columns of M .

The *pmi* further can be explained as the amount of uncertainty in Z_j^t which is removed by knowing Z_i^s i.e. $pmi(Z_i^s; Z_j^t) = H(Z_j^t) - H(Z_j^t|Z_i^s)$. In the open set domain adaptation setting, the target samples from shared classes possess a great deal of similarity to the source samples. Thus, for G and image pairs (x_i^s, x_j^t) , when each image contains the similar object of its pair but has little domain gap (different illuminations, weather, camera conditions, etc.), the random variable constructed by the first of each pair, Z_i^s , will have powerful statistical influence on the random variable for the second one Z_j^t . On the other hand, image pair with dissimilar images will pose a weak statistical relation. Therefore, the known target samples will produce higher *pmi* than unknown samples because of having less difference between the probability of co-occurrence and occurrence and at the same time, more uncertainty removed. We compute the *pmi* (Eq. (10)) of a target sample to every source sample in the batch and consider the highest *pmi* value. The higher the *pmi* of a target sample to a source sample batch means the more probable that it comes from the shared label space C .

For final and fine separation of known and unknown target samples, we integrate a non-adversarial binary discriminator D_2 to G . This discriminator learns to distinguish known and unknown target samples based on the highest and lowest *pmi* with the source domain. To be specific, the discriminator D_2 is trained to yield higher weights for target samples with highest *pmi* than samples with lowest *pmi*. We optimize the binary discriminator D_2 as follows,

$$\begin{aligned} E_{D_2} = -\frac{1}{n_t} \sum_{j=1}^{n_t} & (\log(D_2^h(G(F(x_j^t)))) \\ & + \log(1 - D_2^l(G(F(x_j^t))))). \end{aligned} \quad (11)$$

where, $D_2^h(G(F(x_j^t)))$ and $D_2^l(G(F(x_j^t)))$ denote the prob-

Algorithm 1 Training Procedure

Input: labeled source dataset D_s ; unlabeled target dataset D_t ; Feature extractor F ; main classifier C_1 ; adversarial domain discriminator D_3 ; auxiliary feature discriminator G ; auxiliary source classifier C_2 ; non-adversarial discriminators D_1 and D_2 . F , C_1 and C_2 are pre-trained on D_s .

Output: Trained feature discriminator F and classifier C_1 .

- 1: **while** not converged **do**
- 2: Sample mini-batch from $(x_i^s, y_i^s)_{i=1}^{n_s}$ and $(x_j^t)_{j=1}^{n_t}$;
- 3: Update F , C_2 and D_1 by Eq. (6) + Eq. (7);
- 4: Compute mutual information by Eq. (8);
- 5: Update G by Eq. (9) ;
- 6: **for** $j = 1$:mini-batch **do**
- 7: Compute *pmi* between every source sample $(x_i^s, y_i^s)_{i=1}^{n_s}$ and (x_j^t) by Eq. (10);
- 8: Record the highest *pmi*;
- 9: **end for**
- 10: Record target samples with highest and lowest *pmi*;
- 11: Update D_2 by Eq. (11);
- 12: Compute loss for ‘unknown’ index of C_1 by Eq. (5) using target samples with low weights $w(x_j^t)$;
- 13: Compute losses by Equations (1 - 4);
- 14: Update C_1 , F , and D_3 jointly by computed losses
- 15: **end while**
- 16: **return** Trained C_1 and F .

ability of target samples with highest and lowest *pmi* with the source domain respectively in a batch. Now that D_2 can finely distinguish known and unknown target samples i.e. the output $w(x_j^t) = D_2(G(F(x_j^t)))$ is close to 1 for known samples and close to 0 for unknown samples. This fine separation by D_2 has high confidence because only extremely similar and dissimilar samples are used. The target samples with extreme dissimilarities (i.e. $w(x_j^t)$ close to 0) are plugged in to Equation (4) and recognized as ‘unknown’.

Considering all the above-discussed derivations, we present our proposed adversarial domain adaptation model. We denote the parameters of the F , G , C_1 , D_3 , C_2 , D_1 and D_2 as θ_F , θ_G , θ_{C_1} , θ_{D_3} , θ_{C_2} , θ_{D_1} and θ_{D_2} respectively. The overall

objectives of our proposed method are:

$$\begin{aligned}
 \theta_{C_2}, \theta_{D_1} &= \underset{\theta_{C_2}, \theta_{D_1}}{\operatorname{argmin}} E_{C_2} + E_{D_1} \\
 \theta_G &= \underset{\theta_G}{\operatorname{argmax}} E_{MI_k}, \theta_G = \underset{\theta_G}{\operatorname{argmin}} E_{MI_{uk}} \\
 \theta_{D_2} &= \underset{\theta_{D_2}}{\operatorname{argmin}} E_{D_2} \\
 \theta_{C_1}, \theta_{D_3} &= \underset{\theta_{C_1}, \theta_{D_3}}{\operatorname{argmin}} E_{C_1}^s + E_{C_1}^t + E_{D_3} + E_{ce}^t + E_v^s + E_v^t \\
 \theta_F &= \underset{\theta_F}{\operatorname{argmin}} E_{C_1}^s + E_{C_1}^t - E_{D_3} + E_{ce}^t + E_v^s + E_v^t
 \end{aligned} \tag{12}$$

During back-propagation, we use a gradient reversal layer [16] to calculate the gradient of E_{D_3} efficiently. The job of the gradient reversal layer is to multiply the gradient by a certain negative constant while back-propagating. The gradient reversal phenomenon confirms that the feature distributions over the shared classes C of the source and target domains are made as indistinguishable as possible for the classifier C_1 . The training procedure of DAMI is outlined in Algorithm 1.

IV. EXPERIMENTAL STUDIES

In this section, we describe the datasets, our evaluation details, and discuss the results.

A. Datasets

Office-31 [30] consists of 31 categories in three visually distinct domains, namely: amazon (**A**), DSLR (**D**) and webcam (**W**). This dataset has a collection of samples from **amazon.com**, captured samples from DSLR and web camera. The first ten classes have been chosen as C , and the last ten classes as ‘unknown’ samples in the target domain \overline{C}_t for accomplishing six open set domain adaptation tasks: $A \rightarrow W$, $D \rightarrow W$, $W \rightarrow D$, $A \rightarrow D$, $D \rightarrow A$ and $W \rightarrow A$. **VisDA2017** [67] poses a special domain adaptation setting by focusing on a simulation of synthetic to real images. This dataset has 12 categories. We have selected six classes (bicycle, bus, car, motorcycle, train, and truck) as the shared classes C and the remaining six classes as ‘unknown’ classes in the target domain.

Office-Home [68] comprises of 65 classes in four different domains: Artistic images (**Ar**), Clip-Art images (**Cl**), Product images (**Pr**), and Real-World images (**Rw**). The first ten classes are used as the shared classes C . Except for the next five classes, which are considered private to the source domain, the rest of the classes are selected as ‘unknown’ classes in the target domain. This dataset has 12 domain adaptation tasks: $Ar \rightarrow Cl$, $Ar \rightarrow Pr$, $Ar \rightarrow Rw$, $Cl \rightarrow Ar$, $Cl \rightarrow Pr$, $Cl \rightarrow Rw$, $Pr \rightarrow Ar$, $Pr \rightarrow Cl$, $Pr \rightarrow Rw$, $Rw \rightarrow Ar$, $Rw \rightarrow Cl$ and $Rw \rightarrow Pr$. **ImageNet-Caltech** is composed of ImageNet-1K [69] with 1000 categories and Caltech-256 consisting 256 categories. The common 84 classes are selected as the known or shared classes C , and the remaining classes are considered as the ‘unknown’ class in the target domain [64], [70]. Two open set domain adaptation tasks are performed for this dataset: $I \rightarrow C$ and $C \rightarrow I$.

B. Evaluation Details

We follow the evaluation protocol of the Visual Domain Adaptation (VisDA 2018) Open-Set Classification Challenge in this work. According to the protocol, all the target domain private classes $|\overline{C}_t|$ are assumed to be a unified ‘unknown’ class, and the average per-class accuracy for all the known and unknown $|C| + 1$ classes is the final result. In line with [30], we present the average of per-class accuracy measured on all the known classes and one ‘unknown’ classes ($|C| + 1$) as OS. And, the average per-class accuracy only on the shared or known classes ($|C|$) as OS*.

We have used ImageNet pre-trained ResNet-50[65] for all the tasks except VisDA tasks with customized new layers as the feature generator. For VisDA tasks, we utilize ImageNet pre-trained VGGNet as the backbone. The auxiliary feature discriminator, supplementary classifier and the binary discriminators are designed with fully-connected and batch-normalization layers. All the transformations mentioned earlier are applied in our experiments for the computation of I . The size of all transformed target images are matched to the input size of the main feature generator. We have used SGD with a learning rate of 0.001 for pre-trained layers and momentum of 9. A batch size greater than or equal to 16 is found to be suitable for the effective computation of I in the model. Setting the value of hyper-parameter λ_1 as 10 times greater than the value of λ_2 facilitates the model across various tasks. Setting the values of $\lambda_1 = 1$ and $\lambda_2 = 0.1$ facilitates the *Mutual Information* optimization in our experimental tasks. Readers may adjust the values of the hyper-parameters to their respective tasks empirically.

C. Classification results

In this section, we compare the performance of DAMI against contemporary works. The results for other methods on the tasks of Office-31, Office-Home, and VisDA datasets are taken from [20], [24], and [22]. The results for the tasks of the ImageNet-Caltech dataset are produced using ResNet-50 (as the backbone network) as these results are not available in the literature in this open set domain adaptation setting. In Tables I and II, we report the mean and std. deviation of OS and OS* over three separate runs. Its is worth mentioning, we report only OS accuracy in Table II because of space constraints.

Table I, II, III and IV present the results on the tasks of Office-31, Office-Home, VisDA and ImageNet-Caltech datasets respectively. It is evident that both versions of DAMI outperform all the compared methods on average accuracy and on the majority of the tasks for all the datasets. For closed set methods [28], [17], we observe that the performance lags behind ResNet on some tasks when evaluated following the open set domain adaptation setting. The lag in the performance of these methods compared to non-DA classifier is the result of negative transfer initiated by aligning the whole target domain with the source domain. Thus, the unknown classes are also matched with source data.

Existing open set domain adaptation method lags behind the non-DA classifier ResNet on some tasks on the datasets Office-Home, VisDA and ImageNet-Caltech as reported in

Table I: Classification accuracy (%) of proposed and other domain adaptation methods on Office-31 tasks (ResNet-50).

Approach	Accuracy (%)											
	A → W		A → D		D → W		W → D		D → A		W → A	
	OS	OS*	OS	OS*	OS	OS*	OS	OS*	OS	OS*	OS	OS*
ResNet [65] (2016)	82.5±1.2	82.7±0.9	85.2±0.3	85.5±0.9	94.1±0.3	94.3±0.7	96.6±0.2	97.0±0.4	71.6±1.0	71.5±1.1	75.5±1.0	75.2±1.6
DANN [28] (2016)	85.3±0.7	87.7±1.1	86.5±0.6	87.7±0.6	97.5±0.2	98.3±0.5	99.5±0.1	100.0±0.0	75.7±1.6	76.2±0.9	74.9±1.2	75.6±0.8
RTN [17] (2016)	85.6±1.2	88.1±1.0	89.5±1.4	90.1±1.6	94.8±0.3	96.2±0.7	97.1±0.2	98.7±0.9	72.3±0.9	72.8±1.5	73.5±0.6	73.9±1.4
OpenMax [66] (2016)	87.4±0.5	87.5±0.3	87.1±0.9	88.4±0.9	96.1±0.4	96.2±0.3	98.4±0.3	98.5±0.3	83.4±1.0	82.1±0.6	82.8±0.9	82.8±0.6
ATI [19] (2017)	87.4±1.5	88.9±1.4	84.3±1.2	86.6±1.1	93.6±1.0	95.3±1.0	96.5±0.9	98.7±0.8	78.0±1.8	79.6±1.5	80.4±1.4	81.4±1.2
OSBP [18] (2018)	86.5±2.0	87.6±2.1	88.6±1.4	89.2±1.3	97.0±1.0	96.5±0.4	97.9±0.9	98.7±0.6	88.9±2.5	90.6±2.3	85.8±2.5	84.9±1.3
STA [20] (2019)	89.5±0.6	92.1±0.5	93.7±1.5	96.1±0.4	97.5±0.2	96.5±0.5	99.5±0.2	99.6±0.1	89.1±0.5	93.5±0.8	87.9±0.9	87.4±0.6
TIM [24] (2020)	91.3±0.7	93.2±1.2	94.2±1.1	97.1±0.8	96.5±0.5	97.4±0.7	99.5±0.2	99.4±0.3	90.1±0.2	91.5±0.2	88.7±1.3	88.1±0.9
MTS [22] (2020)	92.4±0.3	96.8±0.8	94.7±0.2	98.2±0.5	97.9±0.2	99.5±0.2	98.9±0.4	100.0±0.0	89.6±0.4	92.0±0.3	89.7±0.2	91.9±0.3
DAMI	96.3±0.2	98.6±0.2	98.2±0.3	100.0±0.4	100.0±0.5	100.0±0.4	98.7±0.1	99.9±0.1	95.7±0.5	97.8±0.4	93.4±0.7	95.8±0.6

Table II: Classification accuracy (%) of proposed and contemporary domain adaptation methods on Office-Home dataset tasks (ResNet-50).

Approach	Accuracy (%)												
	Ar → Cl	Pr → Cl	Rw → Cl	Ar → Pr	Cl → Pr	Rw → Pr	Cl → Ar	Pr → Ar	Rw → Ar	Ar → Rw	Cl → Rw	Pr → Rw	Avg
ResNet [65] (2016)	53.4±0.4	52.7±0.6	51.9±0.5	69.3±0.7	61.8±0.5	74.1±0.4	61.4±0.6	64.0±0.3	70.0±0.3	78.7±0.6	71.0±0.6	74.9±0.9	65.3
DANN [28] (2016)	54.6±0.7	49.7±1.6	51.9±1.4	69.5±1.1	63.5±1.0	72.9±0.8	61.9±1.2	63.3±1.0	71.3±1.0	80.2±0.8	71.7±0.4	74.2±0.4	65.4
ATI [19] (2017)	55.2±1.2	52.6±1.6	53.5±1.4	69.1±1.1	63.5±1.5	74.1±1.5	67.1±1.2	64.5±0.9	70.7±0.5	79.2±0.7	72.9±0.7	75.8±1.6	66.1
OpenMax [66] (2016)	56.5±0.4	52.9±0.7	53.7±0.4	69.1±0.3	64.8±0.4	74.5±0.6	64.1±0.9	64.0±0.8	71.2±0.8	80.3±0.8	73.0±0.5	76.9±0.3	66.7
OSBP [18] (2018)	56.7±1.9	51.5±2.1	49.2±2.4	67.5±1.5	65.5±1.5	74.0±1.5	62.5±2.0	64.8±1.1	69.3±1.1	80.6±0.9	74.7±2.2	71.5±1.9	65.7
STA [20] (2019)	58.1±0.6	53.1±0.9	54.4±1.0	71.6±1.2	69.3±1.0	81.9±0.5	63.4±0.5	65.2±0.8	74.9±1.0	85.0±0.2	75.8±0.4	80.8±0.3	69.5
TIM [24] (2020)	60.1±0.7	54.2±1.0	56.2±1.7	70.9±1.4	70.0±1.7	78.6±0.6	64.0±0.6	66.1±1.3	74.9±0.9	83.2±0.9	75.7±1.3	81.3±1.4	69.6
MTS [22] (2020)	63.7±0.3	58.4±0.3	64.4±0.1	80.6±0.5	74.2±0.4	83.3±0.2	68.4±0.3	71.1±0.3	78.0±0.4	86.0±0.2	79.5±0.2	82.7±0.4	74.2
DAMI	68.1±0.4	63.2±0.6	70.5±0.2	83.7±0.4	83.8±0.2	86.3±0.6	76.7±0.7	80.9±0.4	86.3±0.3	91.2±0.5	87.8±0.7	88.9±0.6	80.6

Table III: Classification accuracy (%) of proposed and other domain adaptation methods on VisDA2017 tasks (VGGNet).

Approach	Accuracy (%)								
	bicycle	bus	car	motorcycle	train	truck	unknown	OS	OS*
ResNet [65] (2016)	40.2	55.4	63.5	70.8	74.1	35.2	45.6	54.9	56.5
ATI [19] (2017)	46.2	57.5	56.9	79.1	81.6	32.7	65.0	59.9	59.0
OSBP [18] (2018)	51.1	67.1	42.8	84.2	81.8	28.0	85.1	62.9	59.2
STA [20] (2019)	52.4	69.6	59.9	87.8	86.5	27.2	84.1	66.8	63.9
TIM [24] (2020)	53.5	69.2	62.2	85.7	85.4	32.5	88.5	68.1	64.7
DAMI	58.1	78.9	88.7	96.8	87.8	42.6	83.1	76.5	75.4

Table IV: Classification accuracy (%) of proposed and other domain adaptation methods on ImageNet-Caltech tasks (ResNet-50).

Approach	Accuracy (%)					
	I → C		C → I		Avg	
	OS	OS*	OS	OS*	OS	OS*
ResNet [65]	75.7	75.1	67.1	67.8	71.4	71.5
BP [16] (2015)	68.9	67.3	61.2	59.0	65.0	63.2
ATI [19] (2017)	71.6	65.9	67.4	65.1	69.5	65.5
OSBP [18] (2018)	63.1	63.4	54.8	53.6	58.9	58.5
STA [20] (2019)	75.3	74.2	68.1	68.3	71.7	71.3
DAMI	81.3	83.8	75.2	78.1	78.2	80.9

tables II, III and IV respectively. These datasets are more challenging as they have a large domain gap compared to the Office-31 dataset. The task performance sacrifice in the contemporary open set domain adaptation methods is caused by the effect of negative transfer during domain adaptation. Though open set domain adaptation methods do not blindly align all target samples to source samples, the negative transfer happens during the known-unknown target sample separation stage before domain adaptation. This issue can be further explained by the results shown in table III. VisDA dataset is way more challenging than other domain adaptation datasets as the adaptation has to happen from synthetic to real images. We observe that there is a considerable gap between the

accuracy of the OS* and OS for the majority of the tasks. The OS* lags behind OS, which means a large number of known images are classified as unknown images. However, besides, increasing the per-class accuracy compared to other methods, DAMI decreases the gap between OS* and OS. Which means optimization of I facilitates the domain adaptation model by imposing better discrimination among similar and dissimilar class features.

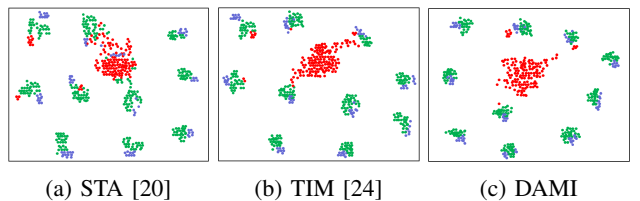


Figure 4: The t-SNE [71] visualization of the last-layer features of the adapted classifiers for the task A → D. Source, target-known and target-unknown samples are shown in green, blue and red colour respectively.

Feature Visualization. We visualize the last layer features in STA, TIM and DAMI on the task A → D in Figure 4. The learned features of some unknown classes in the STA method lie in the near vicinity of the known classes while others are intermingled with known class features. This proves that STA confuses known and unknown samples because of depending

only on the multi-binary classifier. For some cases, TIM improves over the STA method and shows better separation among known and unknown features. On the other hand, for other cases, the unknown class features are even closer to the known classes than STA. This is due to having no access to the source domain during adaptation. The features of DAMI shows a better separation of unknown classes from known classes and well-segregated clusters of aligned known classes of the source and target domain. DAMI leverages the three-step assessment based weighting scheme for this visible well separation of known from unknown classes in the feature space.

Openness. We execute experiments on Office-31 dataset

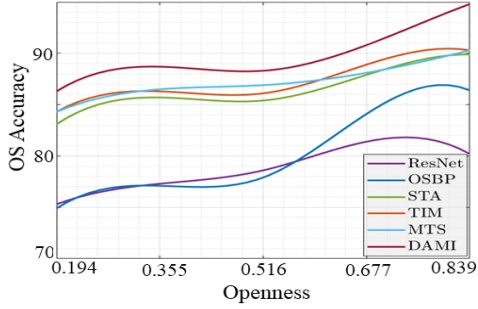


Figure 5: OS Accuracy with respect to different openness levels in the target domain for the task A→D of Office-31 dataset.

to further substantiate the robustness of DAMI in different degree of openness. In Fig. 5, we present the OS accuracy on different levels of Openness, $\mathbb{O} = 1 - |C_s|/|C_t|$ [72]. The superior performance of DAMI in different levels of openness shows that our method is robust for a wide range of openness settings. This compatibility to openness is achieved due to the improved known-unknown samples separation followed by proper adaptation.

Convergence Analysis. We plot the *Mutual Information*

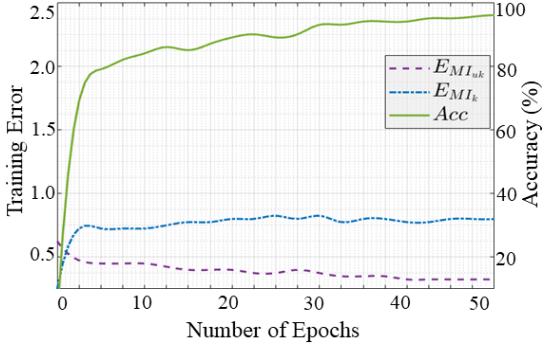


Figure 6: *Mutual Information* optimization training errors $E_{MI_{uk}}$, E_{MI_k} and accuracy with respect to the training epochs for the A→W task.

optimization losses $E_{MI_{uk}}$ (for unknown samples), E_{MI_k} (for known samples) defined by Eq. (9), and the accuracy with respect to the training epochs in the Figure 6. The graph shows that I between known target samples and the source domain is maximized, and I between unknown target samples and the source domain is minimized over the epochs. At the same

time, the classification accuracy maintains a steadily increasing pattern.

D. Visualizing Learned Weights

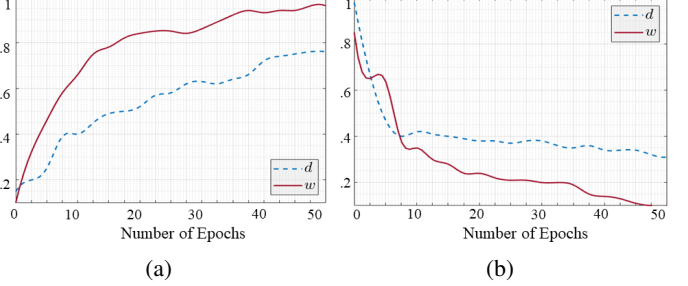


Figure 7: A pictorial illustration of learned weights of (a) known target samples and (b) unknown target samples for the task A→W (Office-31), where d represents the weights generated by discriminator D_1 and w denotes the final instance-level weights assigned to target samples by discriminator D_2 for distinguishing known-unknown target samples and domain adaptation

Figure 7 shows that the final instance-level weight w for known target samples is consistently greater than the primary weight d . Similarly, for unknown samples, w is smaller than d across all epochs. The generated weights d from D_1 struggles to reach near 1 and near 0 values due to the leaky softmax layer in the classifier C_2 . The leaky-softmax assigns a high probability for a logit that has a large probability for a known class. This helps in determining rough domain similarity. However, the leaky-softmax tends to generate element-sum of its output smaller than 1. Due to this tendency, the weights d , that are directly associated with the leaky-softmax element-sum lie in the mid-high and mid-low range. On the other hand, D_2 has no such constraint and is trained on the features of G , which has more discriminative knowledge about known-unknown samples. Thus, the weights w generated from D_2 have high confidence. Also, the weights w has closer to 1 values for known samples and closer to 0 for unknown samples which facilitates the domain discriminator D_3 to adapt better by ignoring unknown samples that possess low weights.

E. Ablation Study

We present the ablation study of DAMI in a building block manner to justify the role of different components in the model. The results of our ablation studies are reported in Table V.

DAN: We start the ablation analysis with the base DAN. This variant does not have any weighting module in the structure except the main feature discriminator F , classifier C_1 and discriminator D_3 . Due to having no prior known-unknown separation module DAN depends on the pseudo decision of C_1 for rejecting target samples as unknown and suffers from a tremendous amount of negative transfer.

CSN + DAN: To help reduce negative transfer by separating known-unknown samples prior to domain adaptation, we place

Table V: Classification accuracy (%) of different variants of DAMI on Office-31 tasks (ResNet-50).

Approach	Accuracy (%)												
	A \rightarrow W		A \rightarrow D		D \rightarrow W		W \rightarrow D		D \rightarrow A		W \rightarrow A		Avg
	OS	OS*	OS	OS*	OS	OS*	OS	OS*	OS	OS*	OS	OS*	
DAN	80.1 \pm 0.3	72.3 \pm 0.8	82.3 \pm 0.6	76.9 \pm 0.9	79.1 \pm 0.6	75.0 \pm 0.8	89.2 \pm 0.6	84.5 \pm 0.8	81.2 \pm 0.4	76.9 \pm 0.6	82.1 \pm 0.8	78.1 \pm 0.5	82.3 77.2
CSN + DAN	91.1 \pm 0.3	90.1 \pm 0.8	92.5 \pm 0.4	92.0 \pm 0.8	96.9 \pm 0.7	95.7 \pm 0.6	95.5 \pm 0.5	94.3 \pm 0.6	88.7 \pm 0.6	87.9 \pm 0.5	89.1 \pm 0.4	91.5 \pm 0.5	92.8 91.9
CSN + MION + DAN	93.3 \pm 0.4	93.2 \pm 0.3	94.5 \pm 0.3	94.7 \pm 0.4	97.4 \pm 0.6	97.6 \pm 0.6	95.7 \pm 0.2	94.8 \pm 0.6	91.1 \pm 0.9	92.3 \pm 0.5	88.3 \pm 0.4	88.1 \pm 0.3	93.3 93.4
DAMI (CSN + MION + FSN + DAN)	96.3 \pm 0.2	98.6 \pm 0.2	98.2 \pm 0.3	100.0 \pm 0.4	100 \pm 0.5	100.0 \pm 0.4	98.7 \pm 0.1	99.9 \pm 0.1	95.7 \pm 0.5	97.8 \pm 0.4	93.4 \pm 0.7	95.8 \pm 0.6	97.0 98.6

supplementary source classifier C_2 and its auxiliary discriminator D_1 . We refer to this version as DAMI without *Mutual Information* optimization module DAN w/ CSN. Though this variant outperforms the previous one, the generated weights d harm the adversarial domain adaptation being influenced by the leaky effect of C_2 (discussed in section IV-D).

CSN + MION + DAN: This variant is implemented without the FSN that has a discriminator D_2 which finely separates known-unknown samples after evaluating point-wise mutual information. Though MION gains the ability to generate discriminative features, it still lacks at generating suitable weights. We use the highest output of G as instance-level soft weights and observe the DAN slightly struggles to differentiate known-unknown as the weights are not yet smooth.

DAMI(CSN + MION + FSN + DAN) outperforms the above-mentioned variants. DAMI is capable of finely separate known-unknown target samples due to integrating FSN. FSN evaluates *pmi* for verifying similarity/dissimilarity of target samples and generates smooth weights through D_2 . In fine, DAMI has access to discerning knowledge of known and unknown domains which assists better in further separation of known-unknown target samples by generating suitable weights before domain adaptation.

V. CONCLUSION

In this paper, we propose a novel Domain Adaptation based on Mutual Information (DAMI) model for addressing the challenge of handling negative transfer in open set domain adaptation. DAMI is capable of separating known from unknown target samples by utilizing the three-step evaluation-verification based weighting module, which leverages the optimization of *Mutual Information* in between similar classes and dissimilar classes. Simultaneously, DAMI aligns features of known target classes to source domain. It is evident from the comprehensive validation on various datasets that DAMI is robust to different level of openness and large domain gaps, and outperforms contemporary works.

REFERENCES

- C. Szegedy, W. Liu, Y. Jia, P. Sermanet, S. Reed, D. Anguelov, D. Erhan, V. Vanhoucke, and A. Rabinovich, “Going deeper with convolutions,” in *Proceedings of the IEEE Conference on Computer Vision and Pattern Recognition (CVPR)*, 2015, pp. 1–9.
- J. Nath Kundu, P. Krishna Uppala, A. Pahuja, and R. Venkatesh Babu, “Adadepth: Unsupervised content congruent adaptation for depth estimation,” in *Proceedings of the IEEE Conference on Computer Vision and Pattern Recognition*, 2018, pp. 2656–2665.
- H. Shimodaira, “Improving predictive inference under covariate shift by weighting the log-likelihood function,” *Journal of statistical planning and inference*, vol. 90, no. 2, pp. 227–244, 2000.
- A. Torralba and A. A. Efros, “Unbiased look at dataset bias,” in *CVPR 2011*. IEEE, 2011, pp. 1521–1528.
- T. Shermin, S. W. Teng, M. Murshed, G. Lu, F. Sohel, and M. Paul, “Enhanced transfer learning with imagenet trained classification layer,” in *Proceedings of the Pacific-Rim Symposium on Image and Video Technology (PSIVT)*, 2019.
- J. Li, K. Lu, Z. Huang, L. Zhu, and H. T. Shen, “Heterogeneous domain adaptation through progressive alignment,” *IEEE transactions on neural networks and learning systems*, vol. 30, no. 5, pp. 1381–1391, 2018.
- J. Li, M. Jing, K. Lu, L. Zhu, and H. T. Shen, “Locality preserving joint transfer for domain adaptation,” *IEEE Transactions on Image Processing*, vol. 28, no. 12, pp. 6103–6115, 2019.
- X. Ma, T. Zhang, and C. Xu, “Deep multi-modality adversarial networks for unsupervised domain adaptation,” *IEEE Transactions on Multimedia*, vol. 21, no. 9, pp. 2419–2431, 2019.
- K. Bousmalis, N. Silberman, D. Dohan, D. Erhan, and D. Krishnan, “Unsupervised pixel-level domain adaptation with generative adversarial networks,” in *Proceedings of the IEEE Conference on Computer Vision and Pattern Recognition (CVPR)*, 2017, pp. 3722–3731.
- E. Tzeng, J. Hoffman, K. Saenko, and T. Darrell, “Adversarial discriminative domain adaptation,” in *Proceedings of the IEEE Conference on Computer Vision and Pattern Recognition (CVPR)*, 2017, pp. 7167–7176.
- M. Liu, T. Breuel, and J. Kautz, “Unsupervised image-to-image translation networks,” in *Advances in Neural Information Processing Systems (NIPS)*, 2017, pp. 700–708.
- Y. Taigman, A. Polyak, and L. Wolf, “Unsupervised cross-domain image generation,” *International Conference on Learning Representations (ICLR)*, 2016.
- K. Saito, K. Watanabe, Y. Ushiku, and T. Harada, “Maximum classifier discrepancy for unsupervised domain adaptation,” in *Proceedings of the IEEE Conference on Computer Vision and Pattern Recognition (CVPR)*, 2018, pp. 3723–3732.
- J. Li, K. Lu, Z. Huang, L. Zhu, and H. T. Shen, “Transfer independently together: A generalized framework for domain adaptation,” *IEEE Transactions on Cybernetics*, vol. 49, no. 6, pp. 2144–2155, 2018.
- P. Haeusser, T. Frerix, A. Mordvintsev, and D. Cremers, “Associative domain adaptation,” in *Proceedings of the IEEE International Conference on Computer Vision (ICCV)*, 2017, pp. 2765–2773.
- Y. Ganin, V. Lempitsky, “Unsupervised domain adaptation by backpropagation,” in *International Conference on Machine Learning (ICML)*, 2015, pp. 1180–1189.
- M. Long, H. Zhu, J. Wang, and M. I. Jordan, “Unsupervised domain adaptation with residual transfer networks,” in *Advances in Neural Information Processing Systems (NIPS)*, 2016, pp. 136–144.
- K. Saito, S. Yamamoto, and Y. U. T. Harada, “Open set domain adaptation by backpropagation,” in *Proceedings of the European Conference on Computer Vision (ECCV)*, 2018, pp. 153–168.
- P. P. Bustos and J. Gall, “Open set domain adaptation,” in *Proceedings of the IEEE International Conference on Computer Vision (CVPR)*, 2017, pp. 754–763.
- H. Liu, Z. Cao, M. Long, J. Wang, and Q. Yang, “Separate to adapt: Open set domain adaptation via progressive separation,” in *Proceedings of the IEEE Conference on Computer Vision and Pattern Recognition*, 2019, pp. 2927–2936.
- S. J. Pan and Q. Yang, “A survey on transfer learning,” *IEEE Transactions on knowledge and data engineering*, vol. 22, no. 10, pp. 1345–1359, 2009.
- D. Chang, A. Sain, Z. Ma, Y.-Z. Song, and J. Guo, “Mind the gap: Enlarging the domain gap in open set domain adaptation,” *arXiv preprint arXiv:2003.03787*, 2020.
- K. Lee, H. Lee, K. Lee, and J. Shin, “Training confidence-calibrated classifiers for detecting out-of-distribution samples,” *arXiv preprint arXiv:1711.09325*, 2017.
- J. N. Kundu, N. Venkat, A. Revanur, and R. V. Babu, “Towards inheritable models for open-set domain adaptation,” *arXiv preprint arXiv:2004.04388*, 2020.

[25] M. Long, Z. Cao, J. Wang, and M. I. Jordan, "Conditional adversarial domain adaptation," in *Advances in Neural Information Processing Systems*, 2018, pp. 1640–1650.

[26] E. Tzeng, J. Hoffman, N. Zhang, K. Saenko, and T. Darrell, "Deep domain confusion: Maximizing for domain invariance," in *Proceedings of the IEEE International Conference on Computer Vision (ICCV)*, 2014.

[27] M. Long, Y. Cao, J. Wang, and M. I. Jordan, "Learning transferable features with deep adaptation networks," *arXiv preprint arXiv:1502.02791*, 2015.

[28] Y. Ganin, E. Ustinova, H. Ajakan, P. Germain, H. Larochelle, F. Laviolette, M. Marchand, and V. Lempitsky, "Domain-adversarial training of neural networks," *The Journal of Machine Learning Research (JMLR)*, vol. 17, no. 1, pp. 2096–2030, 2016.

[29] J. Hoffman, E. Tzeng, T. Darrell, and K. Saenko, "Simultaneous deep transfer across domains and tasks," in *Domain Adaptation in Computer Vision Applications*. Springer, 2017, pp. 173–187.

[30] K. Saenko, B. Kulis, M. Fritz, and T. Darrell, "Adapting visual category models to new domains," in *Proceedings of the European Conference on Computer Vision (ECCV)*. Springer, 2010, pp. 213–226.

[31] X. Wang and J. Schneider, "Flexible transfer learning under support and model shift," in *Advances in Neural Information Processing Systems*, 2014, pp. 1898–1906.

[32] S. J. Pan, I. W. Tsang, J. T. Kwok, and Q. Yang, "Domain adaptation via transfer component analysis," *IEEE Transactions on Neural Networks*, vol. 22, no. 2, pp. 199–210, 2010.

[33] B. Gong, Y. Shi, F. Sha, and K. Grauman, "Geodesic flow kernel for unsupervised domain adaptation," in *2012 IEEE Conference on Computer Vision and Pattern Recognition*. IEEE, 2012, pp. 2066–2073.

[34] K. Zhang, B. Schölkopf, K. Muandet, and Z. Wang, "Domain adaptation under target and conditional shift," in *International Conference on Machine Learning*, 2013, pp. 819–827.

[35] L. Duan, I. W. Tsang, and D. Xu, "Domain transfer multiple kernel learning," *IEEE Transactions on Pattern Analysis and Machine Intelligence*, vol. 34, no. 3, pp. 465–479, 2012.

[36] M. Long, H. Zhu, J. Wang, and M. I. Jordan, "Deep transfer learning with joint adaptation networks," in *Proceedings of the 34th International Conference on Machine Learning-Volume 70*, 2017, pp. 2208–2217.

[37] W. Zellinger, T. Grubinger, E. Lughofner, T. Natschläger, and S. Saminger-Platz, "Central moment discrepancy (cmd) for domain-invariant representation learning," *arXiv preprint arXiv:1702.08811*, 2017.

[38] B. Sun and K. Saenko, "Deep coral: Correlation alignment for deep domain adaptation," in *European Conference on Computer Vision*. Springer, 2016, pp. 443–450.

[39] I. Goodfellow, J. Pouget-Abadie, M. Mirza, B. Xu, D. Warde-Farley, S. Ozair, A. Courville, and Y. Bengio, "Generative adversarial nets," in *Advances in neural information processing systems*, 2014, pp. 2672–2680.

[40] R. Volpi, P. Morerio, S. Savarese, and V. Murino, "Adversarial feature augmentation for unsupervised domain adaptation," in *Proceedings of the IEEE Conference on Computer Vision and Pattern Recognition*, 2018, pp. 5495–5504.

[41] S. Sankaranarayanan, Y. Balaji, C. D. Castillo, and R. Chellappa, "Generate to adapt: Aligning domains using generative adversarial networks," in *Proceedings of the IEEE Conference on Computer Vision and Pattern Recognition*, 2018, pp. 8503–8512.

[42] Z. Murez, S. Kolouri, D. Kriegman, R. Ramamoorthi, and K. Kim, "Image to image translation for domain adaptation," in *Proceedings of the IEEE Conference on Computer Vision and Pattern Recognition*, 2018, pp. 4500–4509.

[43] Y.-C. Liu, Y.-Y. Yeh, T.-C. Fu, S.-D. Wang, W.-C. Chiu, and Y.-C. Frank Wang, "Detach and adapt: Learning cross-domain disentangled deep representation," in *Proceedings of the IEEE Conference on Computer Vision and Pattern Recognition*, 2018, pp. 8867–8876.

[44] S.-W. Huang, C.-T. Lin, S.-P. Chen, Y.-Y. Wu, P.-H. Hsu, and S.-H. Lai, "Auggan: Cross domain adaptation with gan-based data augmentation," in *Proceedings of the European Conference on Computer Vision (ECCV)*, 2018, pp. 718–731.

[45] J.-Y. Zhu, T. Park, P. Isola, and A. A. Efros, "Unpaired image-to-image translation using cycle-consistent adversarial networks," in *Proceedings of the IEEE international conference on computer vision*, 2017, pp. 2223–2232.

[46] P. Russo, F. M. Carlucci, T. Tommasi, and B. Caputo, "From source to target and back: symmetric bi-directional adaptive gan," in *Proceedings of the IEEE Conference on Computer Vision and Pattern Recognition*, 2018, pp. 8099–8108.

[47] J. Hoffman, E. Tzeng, T. Park, J.-Y. Zhu, P. Isola, K. Saenko, A. A. Efros, and T. Darrell, "Cycada: Cycle-consistent adversarial domain adaptation," *arXiv preprint arXiv:1711.03213*, 2017.

[48] J. Li, E. Chen, Z. Ding, L. Zhu, K. Lu, and Z. Huang, "Cycle-consistent conditional adversarial transfer networks," in *Proceedings of the 27th ACM International Conference on Multimedia*, 2019, pp. 747–755.

[49] F. M. Cariucci, L. Porzi, B. Caputo, E. Ricci, and S. R. Bulò, "Autodial: Automatic domain alignment layers," in *2017 IEEE International Conference on Computer Vision (ICCV)*. IEEE, 2017, pp. 5077–5085.

[50] Y. Li, N. Wang, J. Shi, J. Liu, and X. Hou, "Revisiting batch normalization for practical domain adaptation," *arXiv preprint arXiv:1603.04779*, 2016.

[51] Y. Song, L. Yu, Z. Cao, Z. Zhou, J. Shen, S. Shao, W. Zhang, and Y. Yu, "Improving unsupervised domain adaptation with variational information bottleneck," *arXiv preprint arXiv:1911.09310*, 2019.

[52] I. S. Dhillon, S. Mallela, and D. S. Modha, "Information-theoretic co-clustering," in *Proceedings of the ninth ACM SIGKDD international conference on Knowledge discovery and data mining*, 2003, pp. 89–98.

[53] P. Wang, C. Domeniconi, and K. B. Laskey, "Information bottleneck co-clustering," in *Workshop TextMining@ SIAM DM*, vol. 10. Citeseer, 2010.

[54] N. Tishby, F. C. Pereira, and W. Bialek, "The information bottleneck method," *arXiv preprint physics/0004057*, 2000.

[55] A. A. Alemi, I. Fischer, J. V. Dillon, and K. Murphy, "Deep variational information bottleneck," *arXiv preprint arXiv:1612.00410*, 2016.

[56] N. Friedman, O. Mosenzon, N. Slonim, and N. Tishby, "Multivariate information bottleneck," *arXiv preprint arXiv:1301.2270*, 2013.

[57] X. Peng, Z. Huang, X. Sun, and K. Saenko, "Domain agnostic learning with disentangled representations," *arXiv preprint arXiv:1904.12347*, 2019.

[58] R. D. Hjelm, A. Fedorov, S. Lavoie-Marchildon, K. Grewal, P. Bachman, A. Trischler, and Y. Bengio, "Learning deep representations by mutual information estimation and maximization," *arXiv preprint arXiv:1808.06670*, 2018.

[59] W. Hu, T. Miyato, S. Tokui, E. Matsumoto, and M. Sugiyama, "Learning discrete representations via information maximizing self-augmented training," *arXiv preprint arXiv:1702.08720*, 2017.

[60] X. Ji, J. F. Henriques, and A. Vedaldi, "Invariant information clustering for unsupervised image classification and segmentation," in *Proceedings of the IEEE International Conference on Computer Vision*, 2019, pp. 9865–9874.

[61] M. I. Belghazi, A. Baratin, S. Rajeswar, S. Ozair, Y. Bengio, A. Courville, and R. D. Hjelm, "Mine: mutual information neural estimation," *arXiv preprint arXiv:1801.04062*, 2018.

[62] T. Miyato, S.-i. Maeda, M. Koyama, and S. Ishii, "Virtual adversarial training: a regularization method for supervised and semi-supervised learning," *IEEE transactions on pattern analysis and machine intelligence*, vol. 41, no. 8, pp. 1979–1993, 2018.

[63] R. Shu, H. H. Bui, H. Narui, and S. Ermon, "A dirt-t approach to unsupervised domain adaptation," *arXiv preprint arXiv:1802.08735*, 2018.

[64] Z. Cao, K. You, M. Long, J. Wang, and Q. Yang, "Learning to transfer examples for partial domain adaptation," in *Proceedings of the IEEE Conference on Computer Vision and Pattern Recognition (CVPR)*, 2019, pp. 2985–2994.

[65] K. He, X. Zhang, S. Ren, and J. Sun, "Deep residual learning for image recognition," in *Proceedings of the IEEE Conference on Computer Vision and Pattern Recognition (CVPR)*, 2016, pp. 770–778.

[66] A. Bendale and T. E. Boult, "Towards open set deep networks," in *Proceedings of the IEEE Conference on Computer Vision and Pattern Recognition*, 2016, pp. 1563–1572.

[67] X. Peng, B. Usman, N. Kaushik, D. Wang, J. Hoffman, and K. Saenko, "Visda: A synthetic-to-real benchmark for visual domain adaptation," in *Proceedings of the IEEE Conference on Computer Vision and Pattern Recognition Workshops*, 2018, pp. 2021–2026.

[68] H. Venkateswara, J. Eusebio, S. Chakraborty, and S. Panchanathan, "Deep hashing network for unsupervised domain adaptation," in *Proceedings of the IEEE Conference on Computer Vision and Pattern Recognition (CVPR)*, 2017, pp. 5018–5027.

[69] O. Russakovsky, J. Deng, H. Su, J. Krause, S. Satheesh, S. Ma, Z. Huang, A. Karpathy, A. Khosla, M. Bernstein *et al.*, "Imagenet large scale visual recognition challenge," *International Journal of Computer Vision (IJCV)*, vol. 115, no. 3, pp. 211–252, 2015.

[70] Z. Cao, M. Long, J. Wang, and M. I. Jordan, "Partial transfer learning with selective adversarial networks," in *Proceedings of the IEEE Conference on Computer Vision and Pattern Recognition (CVPR)*, 2018, pp. 2724–2732.

- [71] L. Maaten and G. Hinton, "Visualizing data using t-sne," *The Journal of Machine Learning Research (JMLR)*, vol. 9, no. Nov, pp. 2579–2605, 2008.
- [72] W. J. Scheirer, A. de Rezende Rocha, A. Sapkota, and T. E. Boult, "Toward open set recognition," *IEEE transactions on pattern analysis and machine intelligence*, vol. 35, no. 7, pp. 1757–1772, 2012.